UAV Coordination for Autonomous Target Tracking

Richard A. Wise* and Rolf T. Rysdyk†

Autonomous Flight Systems Laboratory

University of Washington, Seattle, WA 98195

This report compares several different methodologies for tracking a moving target with multiple Unmanned Aerial Vehicles (UAVs). Relative position coordination of UAVs is enforced. The comparison considers minimization of heuristics and robustness of performance and stability when the UAVs are exposed to wind and target motion.

Nomenclature

a	Helmsman sensitivity parameter
d	Distance
F_b	Body-fixed frame
g	Gravity constant
r	Radius
s	Arclength position along desired path
$\mathbf{V}$	Velocity
V_a	Airspeed
V_g	Inertial speed (ground speed)
V_w	Windspeed (inertial)
x, y, z	Position coordinates
y_s	Cross-track error
$\kappa(s)$	Curvature of desired path at position s
ϕ	Bank angle
ρ	Radius of curvature
χ	Course
χ_w	Wind direction ('from' convention)
ψ	Heading
ψ_w	Wind vector orientation ($\psi_w = \chi_w + \pi$)
Ψ	Bearing angle of aircraft from the target ('Clock angle' relative to target)

Subscripts and Superscripts

b	Body-fixed reference frame
c	Command
e	Earth reference frame
hat (ˆ·)	Estimate
$icpt$	Intercept
s	Serret-Frenet reference frame
t	Target
w	Wind
$tilde$ (˜·)	Relative parameter(Vehicle - Target)
$minus$ $(\cdot)^-$	A value delayed by one time step

*Research Assistant, Department of Aeronautics and Astronautics, e-mail : wiser2@aa.washington.edu

†Assistant Professor, Department of Aeronautics and Astronautics, email: rysdyk@aa.washington.edu

τ Tangential component (to the orbit)

I. Introduction

Figure 1. Coordinated UAVs Tracking a Target

Figure [1] is an illustration of multiple UAVs coordinating to track a moving target ship. Tracking implies maintaining continuous knowledge of the target's position. Each UAV must maintain its own position while determining the target's position based on onboard sensors. Tracking guidance performance is strongly coupled to the ability of the sensors to determine the target's position. Poor sensor information will lead to a poor track which will lead back to poor sensor information. The combined sensor information of coordinated UAVs provides more accurate target position determination than possible with a single UAV [2]. Thus, there are many ongoing efforts to determine optimal methods to track a moving target with multiple autonomous UAVs.

Cost and reliability are driving factors for using multiple UAVs. The cost of a UAV is largely determined by the quality of its sensor package and position determination package (GPS and INS). However, sending two coordinated UAVs with less complex sensors can lead to a better target track than sending one with a sensor that costs twice as much. Further, the probability of mission success increases as the loss of a single vehicle in a flock of vehicles is less severe than the loss of the only vehicle sent on the mission.

A. The Desired Picture

Figure [2] represents the desired motion of two UAVs orbiting a target. The picture is relative, i.e. as seen from an observer that moves with the target. Notice, that the UAVs maintain a constant distance from the target as well as maintain a constant angular separation, even in the presence of wind. Figure [3] shows the corresponding absolute motion of the UAVs when tracking a target that moves Easterly at constant speed.

B. The Constant Clock Angle Separation Problem

Clock angle is the bearing of the UAV position with respect to the target position:

$$\Psi = atan\left(\frac{y - y_t}{x - x_t}\right) = atan(\frac{\tilde{y}}{\tilde{x}}) \tag{1}$$
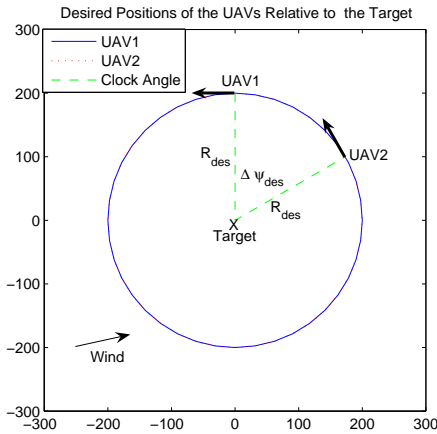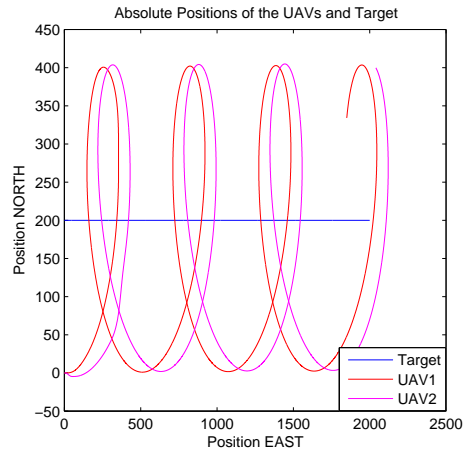
Figure 2. The Desired Relative Picture

Figure 3. The Desired Absolute Picture

The requirement to maintain the clock angle difference between the UAVs while simultaneously tracking a moving target significantly increases the complexity of the tracking problem.

1. Tracking a Moving Target, No Wind

First consider Figure [4(a)] which shows the local velocity vector of a UAV relative to a moving target. The vectors are evenly spaced in time. The UAV rotates counter-clockwise about the target. When the UAV passes the target, the relative speed lessens as does the UAV clock angle rate about the target ($\dot{\Psi} = (|(\mathbf{V}_{uav} - \mathbf{V}_t|)_\tau)/r$). This is seen in Figure [4(a)]: the vectors seem bunched up. When the UAV has rotated past the front of the target, its relative speed increases to include the target motion in the opposite direction. This higher speed results in higher clock angle rate. This is visible in Figure [4(a)] as the vectors spreading apart.

2. Tracking a Stationary Target With Wind

Now consider the problem of target tracking in the presence of a wind field, as shown in Figure [4(b)]. Here a UAV orbits a stationary target, but with a constant wind from right to left. In Figure [4(a)], the velocity vectors are evenly spaced in time, but are bunched up when the vehicle travels against the wind and spread out when the vehicle is with the wind. The relative speed effect is *exactly* the same as caused by target motion ($\dot{\Psi} = (|(\mathbf{V}_{uav} - \mathbf{V}_w|)_\tau)/r$). Unlike the target, however, the wind also affects the vehicle dynamics. Increased ground speed due to wind will cause an additional increase in bank angle due to the coordinated coupling of heading rate and bank angle. High wind speeds will cause bank angle limit saturation even when equivalently fast targets do not.

3. Tracking a Moving Target With Wind

Combining the effects of a moving target with wind may render a real UAV, with bank angle limits and response dynamics, incapable of maintaining or even converging to the desired circular orbit in Figure [2].

For example, assume that the wind is in a direction opposite the motion of the target. As the UAV passes the target, its ground speed is reduced by the wind velocity. This results in a lesser clock angle rate. Assuming that the ground speed of the UAV remains higher than the target, the UAV should be able to continue its orbital path. As the UAV rounds the target, its ground speed will increase by the wind speed resulting in a higher clock angle rate necessary for continued orbit. The bank angle of the UAV must increase to accommodate, possibly to saturation. Again, this is not only due to the UAV's increased relative speed with respect to the target, but also due to its increased inertial speed due to the wind. This may cause the UAV to lag behind the target, diverging from the orbit, until the UAV turns back into the wind to catch back up with the target. In other words, the control authority of the UAV is increased when it is not needed and
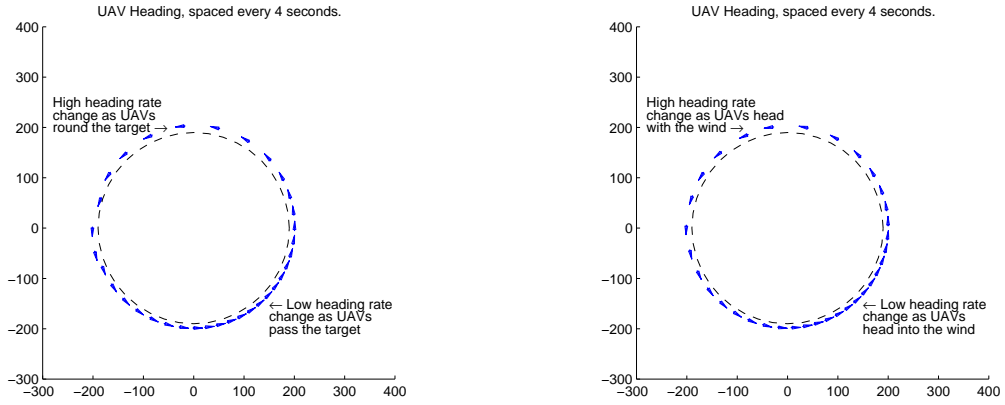
(a) Effect of Target Motion On Course Rate of Change   (b) Effect of Wind On Course Rate of Change

Figure 4. Relative Motion Effects on Course Rate of Change

degraded just it is. Of course, if the wind were to go in the opposite direction, everything would be easier, but this cannot be expected in general.

4. Coordinated Tracking of a Moving Target With Wind

The clock angle rate is now given by:

$$\dot{\Psi}^2(t) = \frac{\left(V_g(t)^2 + V_t^2 + 2V_g(t)V_t(t)\sin(\Psi(t) - \psi_t(t))\right)_\tau}{\tilde{r}(t)^2} \tag{2}$$

For coordinated tracking, the clock angle separation must first be achieved and then held constant by matching the clock angle rate of change. Note that clock angle rate varies with target velocity, wind velocity, and clock angle. The control logic must account for each of these factors, within the bounds of aircraft performance (bank angle limits) and behavior (dynamics). This must be done simultaneously with tracking the target.

5. Coordinated Tracking - Open Issues

Finally, inherent in multi-vehicle coordination are two other open issues: inter-vehicle communication and collision avoidance. As these issue are not addressed by this paper, it is assumed that for the purposes of comparison, the communication is perfect and collision avoidance is handled by altitude separation.

II. Kinematic Coordinated Turn UAV Model

As with most conventional aircraft, the UAV control problem would normally involve the following degrees of freedom : airspeed, aerodynamic side-slip angle, turn rate, and flight path angle. The available aerodynamic control surfaces for rotation about the three body axes are the ailerons, elevator, and rudder. The propulsion (throttle) remains and will be assumed to work in conjunction with the elevator to control altitude and airspeed. Since this control problem addresses guidance at constant altitude, it will be assumed that airspeed and altitude can be held (or controlled) independent of lateral-directional commands.

Aileron and rudder signals are combined to zero sideslip providing a "truly banked turn" or a 'coordinated turn'. Turn coordination relates the bank angle and turn rate, kinematically, as follows:

$$\tan\phi = \frac{V_g}{g}\dot{\psi} \tag{3}$$

In Equation [3], note again the difference between wind and target motion. Only wind will effect this kinematic scaling between heading rate and bank angle.

4

To account for aircraft dynamics, a command in airspeed will be assumed to have a first order response by the UAV as follows:

$$V_a = \frac{1}{s+1} V_c \qquad (4)$$

A command saturation of $\pm 20\%$ of nominal speed is used.

Bank angle response shows a first order behavior:

$$\phi = \frac{1}{0.3s + 1} \phi_c \qquad (5)$$

A bank angle rate limit of $\pm 45\ deg/s$ is used as well as a command saturation of $\pm 45\ deg$.

We will simply relate navigation over the ground via a flat earth model. As we will allow for wind, we distinguish between heading (horizontal orientation of the body frame) and course (horizontal orientation of the UAV over ground, i.e. in the inertial frame).

Figure [5] is a diagram of inputs and outputs relating the control logic to the UAV motion. Note that the the control logic will take in (at least) UAV and target ground velocity (or position) and orbit parameters (radius and UAV clock angle separation) and output a course rate command and velocity command. Sensed wind information may also be used by the controller (not shown). Also note the necessity of vehicle communication: the speed and clock angle of *both* UAVs are inputs.
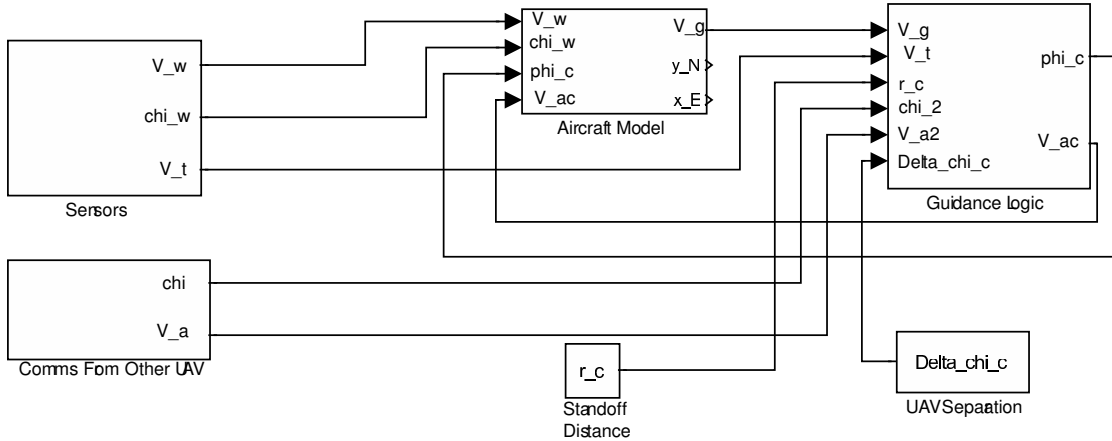
Figure 5. Information Flow To and From the Guidance Logic

6. Comparative Simulations

For all simulations, two UAVs will be required to coordinate positions while tracking the following target speed profiles:

1. No Wind, No Target Motion (control)

2. Constant wind, Wind Speed:UAV Speed = 0.2, Direction: from West, No Target Motion

3. No Wind, Slow Target Profile in Figure [6]

4. No Wind, Fast Target Profile in Figure [7]

5. Wind Speed:UAV Speed = 0.2, Wind Direction with Target, Slow Target Profile as in Figure [6]
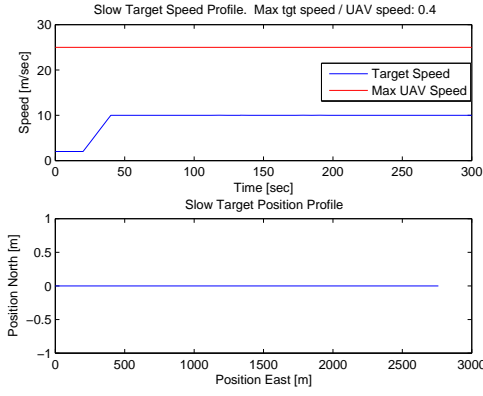
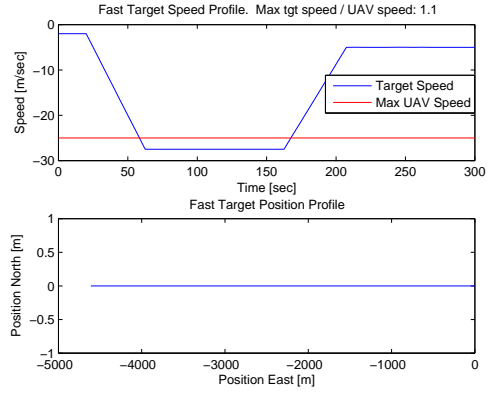6. No Wind, Target Turning in Figure [8]

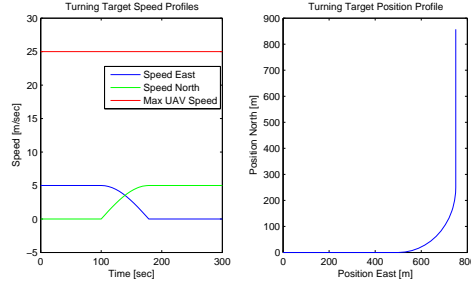**Figure 6. Slow Target**

Figure 7. Fast Target

Figure 8. Turning Target

III.   Method 1 : Helmsman Behavior Based Guidance Law

A.   Description

The first method is an extension of path following as developed here by Rysdyk [5]. In this work, converging back to the desired path consists of stabilizing two degrees of freedom to zero: course angle error, and cross track distance. The path geometry to be followed is determined based on the target current position and heading as well as a standoff distance.

Deviations from this path produce the course angle error and cross track distance. "Good Helmsman" behavior is employed, so-called as it smoothly transitions from current path to the desired path by *simultaneously* bringing cross track distance and course angle error to zero:

$$\sigma_s = (\tilde{\chi} - \chi_s)\frac{e^{-ay_s/2} - 1}{e^{-ay_s/2} + 1} \tag{6}$$

The output, σ_s, is the commanded relative course with gain a. A PD control relates this to the course rate:

$$
\begin{aligned}
\chi_s &= s^-\kappa_1 \\
\tilde{\chi}_s &= \tilde{\chi} - \chi_s \\
y_s &= \int_0^t (V_c \sin(\tilde{\chi}_s) d\tau \\
s &= \int_0^t (V_c \cos(\tilde{\chi}_s)(1 - y_s^-\kappa_1)) d\tau \\
\dot{\psi}_c \approx \dot{\chi}_c &= \left(k_p(\sigma_s - \tilde{\chi}_s) + k_i \int_0^t (\sigma_s - \tilde{\chi}_s) d\tau \right) - V_c\kappa_2
\end{aligned}
\tag{7}
$$

6

Here, κ_1 is the command nominal path curvature ($1/r_c$) and κ_2 is the 'adjusted' path curvature. For two UAV coordination, the lead aircraft normally holds a constant stand-off distance from the target so κ_1 and κ_2 are equal. Based on the clock angle separation error (using another "Good Helmsman" transition function), the follower aircraft adjusts κ_2 as well as adjusting the cross track error used to calculate σ_s: $y_s = y_s + (1/\kappa_2 - 1/\kappa_1)$. Optionally, both aircraft adjust radius oppositely (one increase, other decrease). Also, both aircraft speeds adjust (one up, one down) when speed control is available. This provides the necessary additional degree of freedom to achieve a desired angular separation between the two UAVs.

B.   Simulations
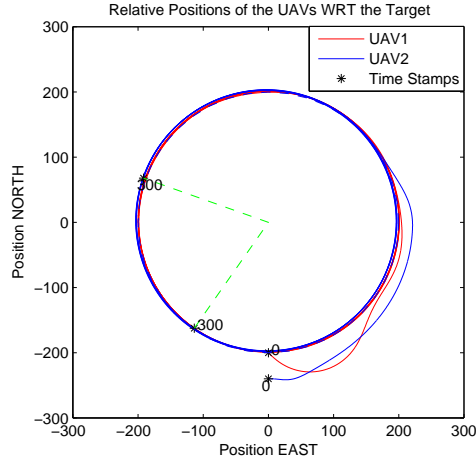
Figure 9. Helmsman: Tracking a Fixed Target With an Initial Condition Offset

Figures [9-15] resulted as the target and wind velocity profiles were changed per Section [II.6]. In each figure, UAV1 is the 'lead' UAV and UAV2 is the 'follower'.

In Figure [9], UAV1 has the initial heading of -45 degrees. In comparison to Figure [2], UAV1 should have a heading of zero degrees at this point in the orbit. An orbit correction occurs as a result, and UAV1 settles on the desired orbit. UAV2 has an initial distance from the target further than the commanded orbit radius of 200 meters. Further, the clock angle between UAV1 and UAV2 is zero whereas the commanded relative clock angle is 75 degrees. UAV2 also corrects and settles on the desired orbit with a correct separation clock angle. This method is able to correct for initial condition errors. Further simulations will all start with both UAVs having heading angles of 0 degrees and initial positions 200 meters to the South of the target.

Figure [10] shows that this method works when the target is stationary and no wind is present. Figure [11] demonstrates the effect of wind, which is clearly minor. A regular oscillation occurs for the relative clock angle between the UAVs, but remains bounded to within 2% of the command.

In Figure [12], target forward speed has a similar effect on the relative clock angle as the wind, i.e. a small, regular oscillation. Wind can be seen to skew the orbit patterns of the UAVs in Figure [13]. The compensation of UAV2 is also apparent as UAV2s radius regularly changes. The wind has also caused the clock angle to be affected in a regular pattern. The overshoot has increased to approximately 25%.

In Figure [14], the UAVs are too slow to remain near the target and fall behind. Considering the logic in Equation [7], and noting that cross-track error will grow large as the target distance increases, the heading rate command will quickly grow and saturate the bank angle commands of the two UAVs. Each spins about a tight orbit. Even when the target slows, the command does not relieve enough for UAV1 due to the integral action winding up the command, and UAV1 continues to spin. UAV2 however, modifies its cross track error based upon the difference in clock angle. UAV1's clock angle from the target is nearing a
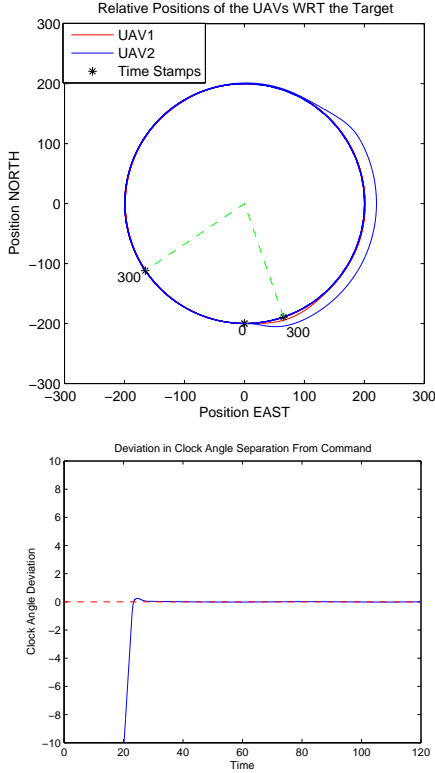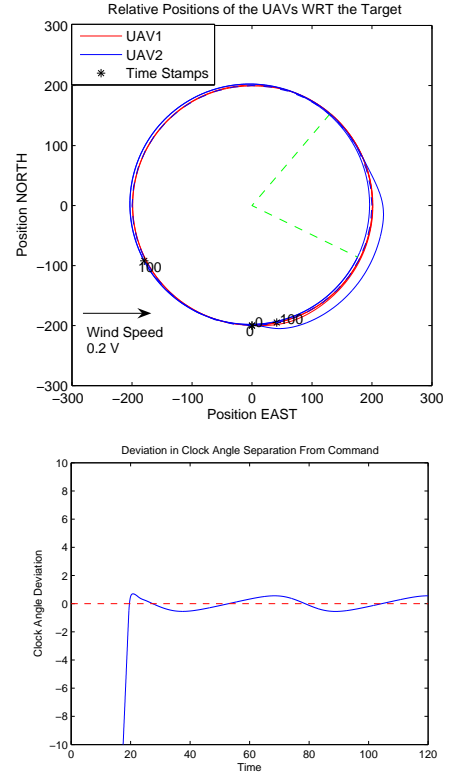
Figure 10. Helmsman: Tracking a Fixed Target

Figure 11. Helmsman: Tracking a Fixed Target With Wind

constant, but the clock angle between UAV1 and UAV2 is increasing. This creates an increasing error signal and causes UAV2 to reduce its cross track error signal, desaturating the heading rate command.

Finally, Figure [15] demonstrates the UAV's ability to follow a target through a turn.

IV. Method 2 : Lyapunov Vector Field Guidance Law

A. Description of the Vector Field

The second method builds upon the work done by Lawrence and Frew [3]. The guidance of the UAV to the observation orbit is determined by building a vector field that has a stable limit cycle centered on the target position. The governing equations are as follows:

$$r = \sqrt{\tilde{x}^2 + \tilde{y}^2}$$
$$vx = -\tilde{x}(r^2 - r_c^2) - 2rr_d\tilde{y}$$
$$vy = -\tilde{y}(r^2 - r_c^2) + 2rr_d\tilde{x}$$
$$\chi_{comVF} = atan2(vy, vx)$$
$$\Delta_{chi\_com} = \chi_{comVF} - ang(\tilde{\vec{V}}) \tag{8}$$

Figures [16-18] visualize this vector field. Figure [16] shows the vector field surrounding a stationary target. It is clear that a path following the field vectors from any point will end up on a circle of radius equal to the specified stand-off distance (shown in black).

To understand how the target motion effects the velocity field, the rate of change of the gradient due to the target can be determined as follows: The area around the target is discretized into points at relative coordinates (i, j) (i.e. target relative location is (0,0)). The gradient is calculated at each discrete point
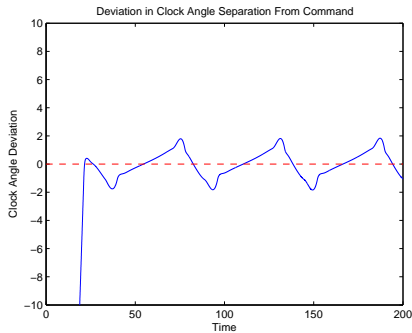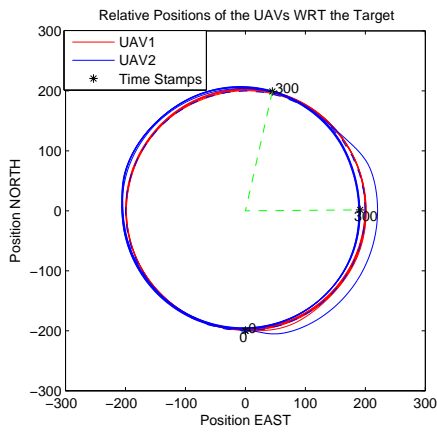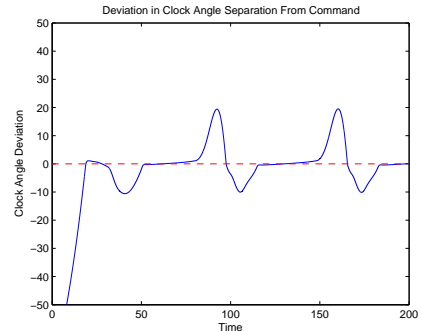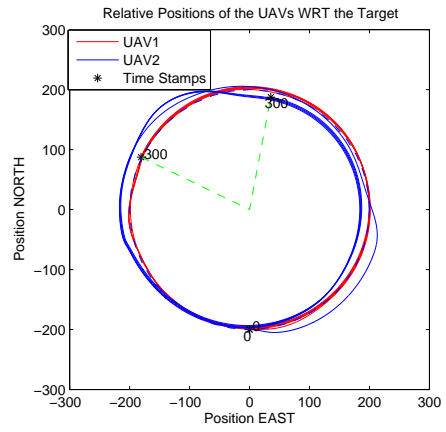
Figure 12. Helmsman: Tracking a Slow Target
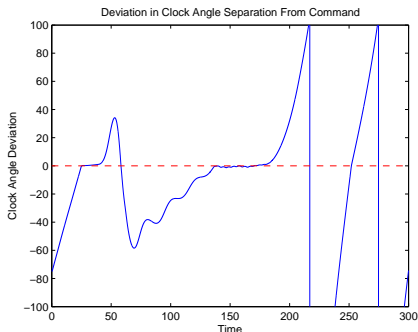

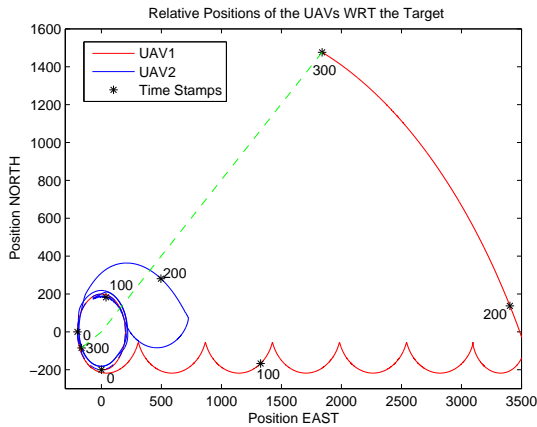**Figure 13. Helmsman: Tracking a Slow Target With Wind**

Figure 14. Helmsman: Tracking a Fast Target
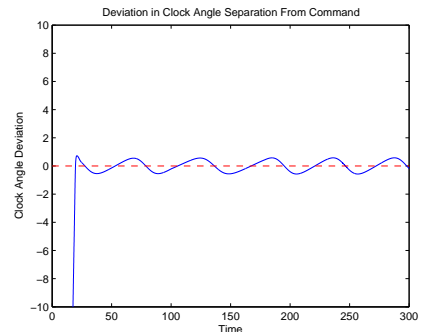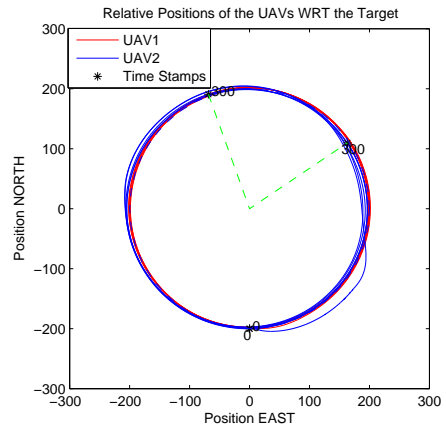

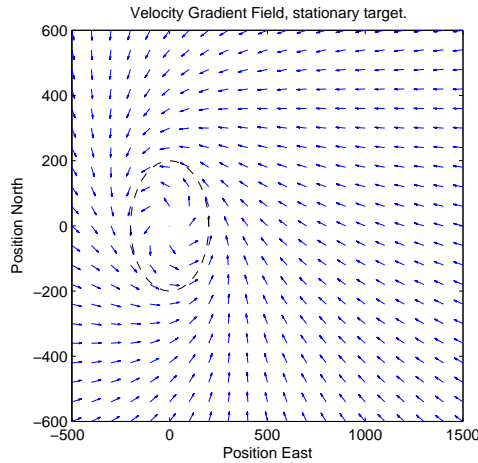**Figure 15. Helmsman: Tracking a Turning Target**

Figure 16. Stationary Target Vector Field

resulting in the direction of the field vector $\chi_{(i,j)}(t)$. A new gradient vector is calculated at the same points (i,j), but with target position delayed in time by ΔT, resulting in a new field angle $\chi_{(i,j)}(t - \Delta T)$. Rate of change is thus:

$$\dot{\chi} = \frac{\chi_{(i,j)}(t) - \chi_{(i,j)}(t - \Delta T))}{\Delta T} \tag{9}$$

Figures [17-18] show the vector field locally surrounding a target moving Easterly. In each figure, a color map is used to indicate vector rotational rates as a percentage of the maximum possible heading rate. Far from the target, the color is constant and represents $\dot{\psi} < 0.25\dot{\psi}_{max}$. Each subsequent shade darkening of the map indicates an increase of $0.25\dot{\psi}_{max}$. A dark, dashed line indicates the relative orbit around the target. The maximum heading rate is based on Equation [3]. A heading rate of greater than 17.7 deg/sec will saturate the bank angle command, set at 45 degrees.

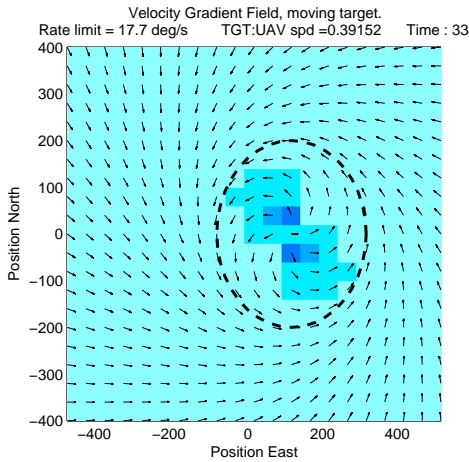In Figure [17], the target's speed is 43% that of the UAV's. No shade increase appears along the or-

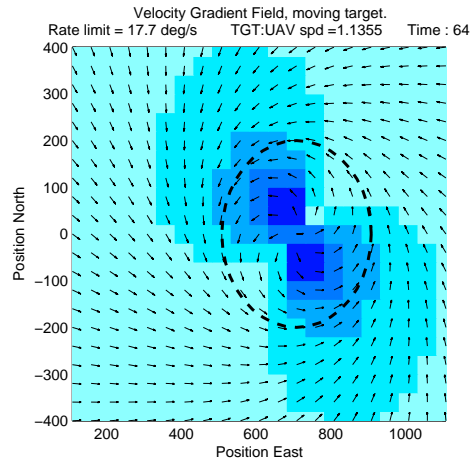**Figure 17. Slow Target Vector Field**

Figure 18. Fast Target Vector Field

bit and thus the maximum command along the orbit remains less than $0.25\dot{\psi}_{max}$. In Figure [18], the target has speed of 110% that of the UAV. And yet, along the orbit, the shade has increased by only two increments indicating a command of $\dot{\chi}_c < 0.75\dot{\psi}_{max}$. Indeed, the command does not increase to greater than $\dot{\psi}_{max}$ unless the UAV is well within the specified standoff distance. Thus, assuming that no wind is present,

10

the angle command given by the vector field is within the capability of the UAV to follow for all target speeds for which the UAV can orbit the target.

B. Application of the Vector Field for Control Guidance

To extend the vector field angle output to the required logic output start with:

$$\dot{\psi}_c \approx \dot{\chi}_c = k_p \Delta_{chi\_com} + k_d \, ang(\tilde{\vec{V}}) \tag{10}$$

To ensure the heading rate command is still within the bounds of the UAV capability, the proportional constant, k_p, is kept less than unity and the derivative term is set to only reduce the heading rate command.

To be able to follow a target that goes faster than the UAV, a second command is generated:

$$\dot{\chi}_{ct} = k_2 \Delta \left(ang(\tilde{\vec{V}}) - ang(\theta_{tan}) \right) \tag{11}$$

where $ang(\theta_{tan})$ is the angle of a line that connects the current UAV position to the tangent of a circle, centered on the target postion, of radius equal to the specified stand-off distance.

However, this command is heavily weighted, as a function of target distance, such that it only has an effect when the UAV is distant from the target. This is the case when Equation [10] is insufficient to maintain the UAV at stand-off distance, such as when the UAV becomes slower than the target. Conversely, the basic vector field command is weighted oppositely. This ensures that the vector field command is used whenever the UAV is near, and can keep up with, the target. The weighting functions are used as transitions to avoid hard switches.

C. UAV Coordination

Assuming UAV relative velocity remains positive, angular separation can be achieved by varying UAV speed proportional to the angular separation error:

$$V_c = V_{c0} + kR_c(\Psi_c - (\Psi_1 - \Psi_2)) \tag{12}$$

Note that k is negative for UAV1 and positive for UAV2. Therefore, the vehicles will change speeds equally but oppositely (one will increase, the other decrease).

At high relative speeds, it becomes much more difficult to maintain large clock separation due to the high heading rate changes. To compensate, Ψ_C is reduced as a function of increasing target speed. If the target becomes faster than the UAV, accurate tracking becomes less of a concern than losing too much ground and therefore losing any track of the target. In this case, the angular compensation is turned off and the speed command is increased to maximum speed in an attempt to minimize distance gained by the target.

D. Simulations

Figures [19-24] resulted as the target and wind velocity profiles were changed per Section [II.6]. In each figure, UAV1 is the 'lead' vehicle and UAV2 is the 'follower'.

In Figure [19], it is clear that this method can meet the clock angle requirement while loitering around a stationary target with no wind present. Note that this method reaches a zero deviation about 10 seconds slower than the Helmsman method. Figure [20] demonstrates the effect of wind. An undamped oscillation occurs for the relative clock angle between the UAVs, but remains bounded to within 2 degrees of the command, only a slightly larger oscillation amplitude than the Helmsman method.

In Figure [21], target forward speed has a similar effect on the relative clock angle as the wind, i.e. an undamped oscillation. Note that the amplitude is slightly less than for the Helmsman method. Wind can be seen to skew the orbit patterns of the UAVs in Figure [22], but has much less of an effect than it does on the Helmsman method.
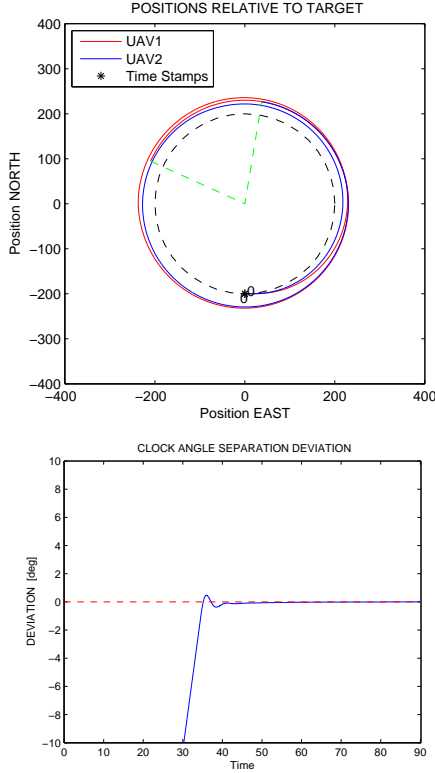
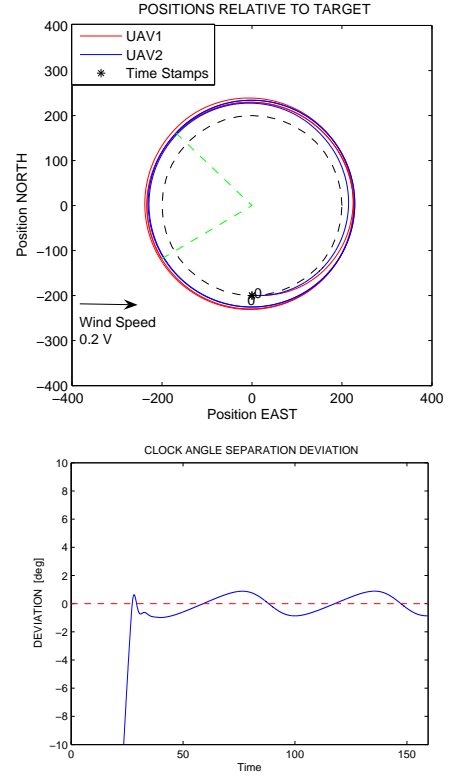**Figure 19. Lyapunov: Tracking a Fixed Target**

Figure 20. Lyapunov: Tracking a Fixed Target With Wind

In Figure [23], the UAVs are too slow to remain near the target and they fall behind. A line tangent to the UAVs' backward-drawing path can be seen to fall ahead of the westerly moving target by about 300 meters. This is due to the 'fast target' compensation described by Equation [11]. When the target speed drops below the speed of the UAV near time 170 (see Figure[7]), the UAVs again gain ground on the target and transition back to their orbit. It should be noted that this result was obtained only after making the following modification:

Equations [8] and [10] show that the heading rate command depends on the angle of the relative velocity vector. For $K > 1$

Case 1: Let $\vec{V}_{rel1} = \vec{V}_{UAV} - \vec{V}_{tgt}$, where $|\vec{V}_{UAV}| = K \times |\vec{V}_{tgt}|$.
Case 2: Let $\vec{V}_{rel2} = \vec{V}_{UAV} - \vec{V}_{tgt}$, where $|\vec{V}_{tgt}| = K \times |\vec{V}_{UAV}|$.
$\rightarrow |\vec{V}_{rel1}| = |\vec{V}_{rel2}|$ but for $ang_{rel} = ang(\vec{V}_{rel})$, $ang_{rel2} = ang_{rel1} + \pi$.

When Case 1 is used regardless of the relative speed, the result is an injection of an extra π in the calculated heading angle as the target speed increases beyond the UAV's speed. The result saturates the error command and results in significant overshooting. As a solution to this problem, note that the relative angle can also be calculated by determining the difference in course angles:

$$ang_{rel-b} = ang(\vec{V}_{UAV}) - ang(\vec{V}_{tgt})$$

In all results shown for this method, ang_{rel-b} is used preferentially over ang_{rel} at target speeds faster than the UAV. The transition between the two angle commands is provided by a weighting function resulting in a smooth relative angle command without overshoot.
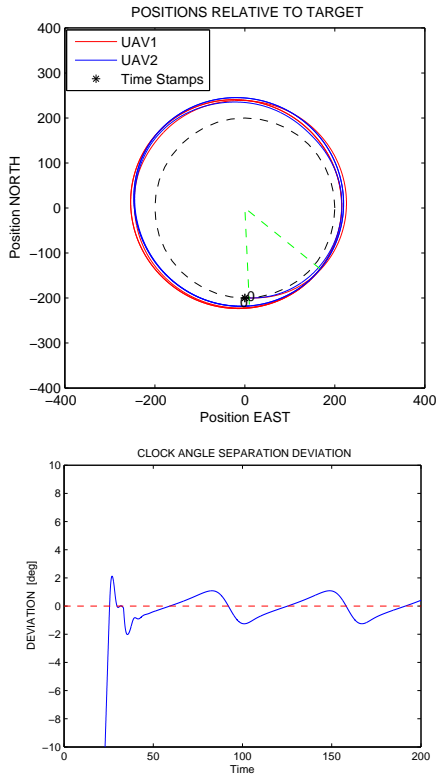
12

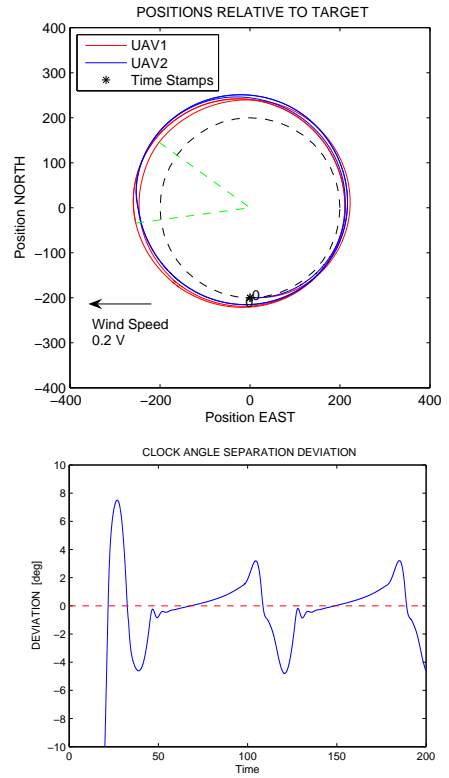**Figure 21. Lyapunov: Tracking a Slow Target**

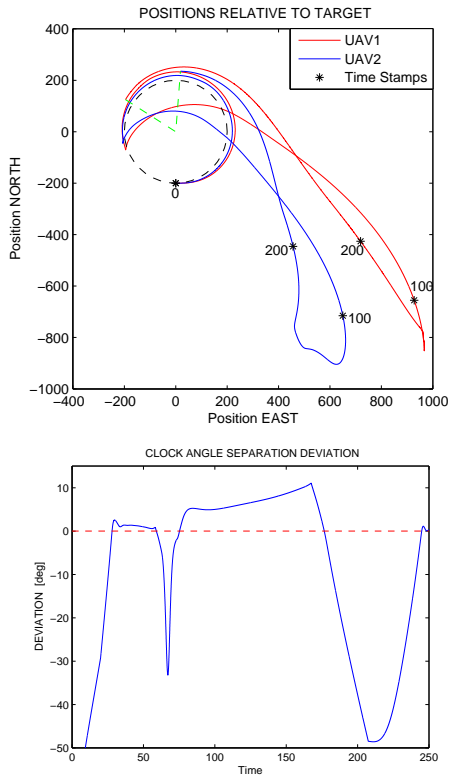**Figure 22. Lyapunov: Tracking a Slow Target With Wind**

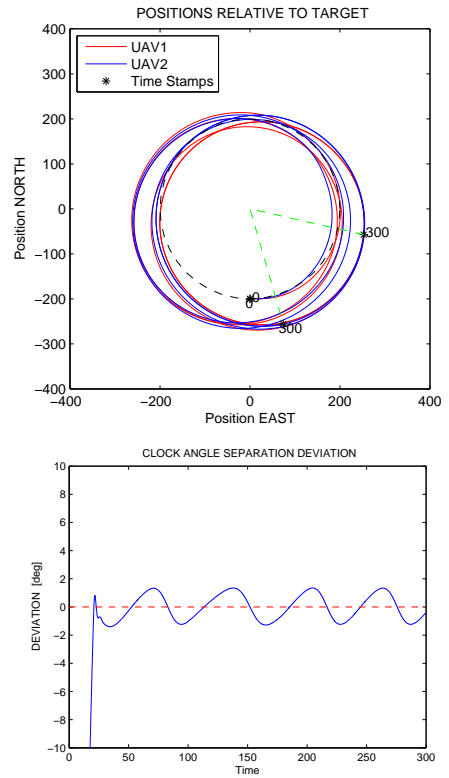
Figure 23. Lyapunov: Tracking a Fast Target

Figure 24. Lyapunov: Tracking a Turning Target

13

Finally, Figure [24] shows that the UAVs can follow a target through a turn. Note that the relative orbits of the UAVs shift due to the target turning. In [3], it is shown that the radius can be made nearly constant by modifying the vector field with sensed target and wind velocities. This can also be accomplished by wrapping an outer-loop, proportional control around the vector field command that reduces the error between the relative orbit heading and the vector field heading.

V. Method 3 : Controlled Collective Motion

A. Description

The third method builds upon the work done by Klein and Morgansen [4]. In [4], the guidance of unit speed planar kinematic unicycles is commanded such that the centroid of the 'flock' of oscillators corresponds with the moving target position. Our extension on this work applies this method to UAV limits and dynamics, again attempting to impose a constant angular separation between two UAVs. The basic equations for the control of $\dot{\chi}_j$, $j = 1 \ldots m$, where m is the number of UAVs, are:

$$
\begin{aligned}
\dot{\chi}_j &= u_1 + u_2 + u_3 \\
u_1 &= uspac_j \\
u_2 &= \frac{K}{n}\left(\frac{d}{d\chi_j}(vek_j)u1_j\right) \\
u_3 &= -\frac{K}{n}\left(vek_j\frac{d}{d\chi_j}(tek_j)u2_j\right)
\end{aligned}
\tag{13}
$$

Where:
$uspac_j$ calculates the control necessary to achieve a specified distance from UAV_j to the centroid,
$\frac{K}{n}\left(\frac{d}{d\chi_j}(vek_j)u1_j\right)$ describes the control necessary to match the target and centroid speed,
$-\frac{K}{n}\left(vek_j\frac{d}{d\chi_j}(tek_j)u2_j\right)$ describes the control necessary to match the centroid direction of travel with that of the target.

Knowing also that K contained within Eqn [13] is an adjustable control gain, immediate insight is gained. Note that if K is zero, no control authority is given to match the centroid velocity (speed and direction) with the velocity of the target and thus we cannot expect the UAVs to track any target that moves. Note also that if $K \to \infty$, no control authority is given to keep the UAVs at a specified distance from the centroid. Thus nothing prevents the UAVs from heading, in radially opposite directions, towards infinity, as the centroid will still remain locally near the target. There is an explicit tradeoff between maintaining the UAVs at a specified distance from the centroid and matching centroid velocity with target velocity.

This tradeoff is of significant issue if there are only two vehicles. In fact, there is no hope of perfectly tracking the target velocity. Figure [25] shows that the UAVs, simply modeled as oscillators, increasingly lag behind a target that is only one tenth as fast as the UAV. If the UAV number increases to three, this problem is alleviated as the centroid of three vehicles can be adjusted either to the left or right of the centroid of two. This extra authority over the centroid position, based on the position of the third vehicle, is enough to drive the centroid to meet the target and stay there as in Figure [27]. Note however, in the case of two UAVs, the orbit spacing is always maintained by default (the UAVs are always separated by a clock angle of 180° with respect to the centroid), as long as the centroid is maintained on the target position. In the case of three vehicles, the 'adjustment' above to keep the centroid tracking the target penalizes the spacing requirement. As each vehicle will have differing distances from the centroid, each will also have differing rotational rates around the centroid. This will result in non-constant clock angle separation as in Figure [26].

As the problem at hand focuses on two vehicles, a solution to target tracking must be found in order to further consider this method. Consider a *swarming* function, similar to the tangent function of Section [IV.B]. Recall that this function directs the UAV along a path tangent to a circle, centered on the target position, of radius equal to the specified standoff distance. This command is combined with the centroid commands to give:

$$
\dot{\chi/}_{j\,tot} = (1 - e^{\frac{-dc}{K}})\delta_{\chi_{jt}} + e^{\frac{-dc}{K}}\dot{\chi}_j \qquad j = 1, 2
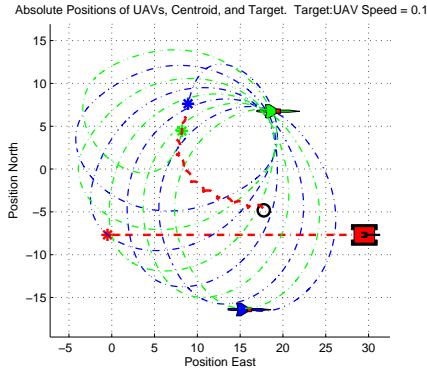\tag{14}
$$

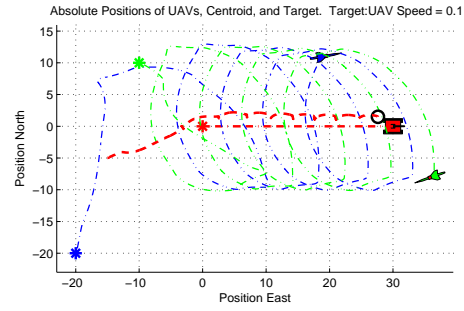**Figure 25. Centroid : Two Oscillators Tracking a Target**

Figure 26. Centroid : Tracking With a Tangent Swarming Function
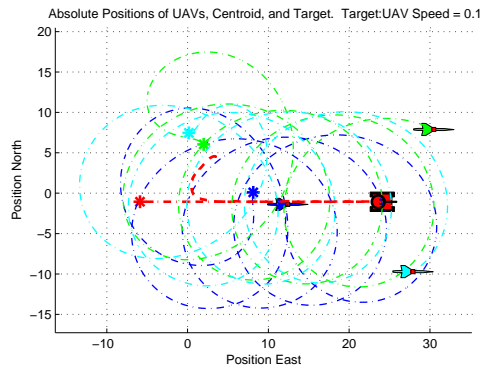

Figure 27. Centroid : Three Oscillators Tracking a Target

Where d_c is the distance from the centroid to the target and K is an adjustable gain.

Equation [14] swarms, or brings all of the UAVs toward the target by setting the commanded heading rate to zero only if the vehicle heading is pointing along the tangent line to the target. The exponential weighting functions avoid the use of switching by providing the emphasis on the original function (trade off vehicle spacing and centroid-target convergence) only when the distance from the centroid to the target is small. This implies that one can reduce the gain in Equation [13] to achieve good distance separation as the swarming function complements the centroid-target convergence by definition. See Figure [26].

B. Simulations

Figures [28-33] resulted as the target and wind velocity profiles were changed per Section [II.6]. In each figure, the path of UAV1 is in blue, the path of UAV2 is in green, and the path of the centroid is in red.

Figure [28] demonstrates the loitering capability of this method. A slight oscillation in the clock angle occurs. The wind, as seen in Figure [29], significantly alters the orbit patterns of the UAVs. This moves the centroid away from the target position, detrimentally to the clock angle separation.

Figures [30 - 33], as opposed to Figures [25 - 26], demonstrate the considerable effect of adding kinematics and dynamics to the oscillator model upon which this method is based. In each case, the variations of the clock angle separation with respect to the target is quite large. This is due to the 'traveling' of the centroid
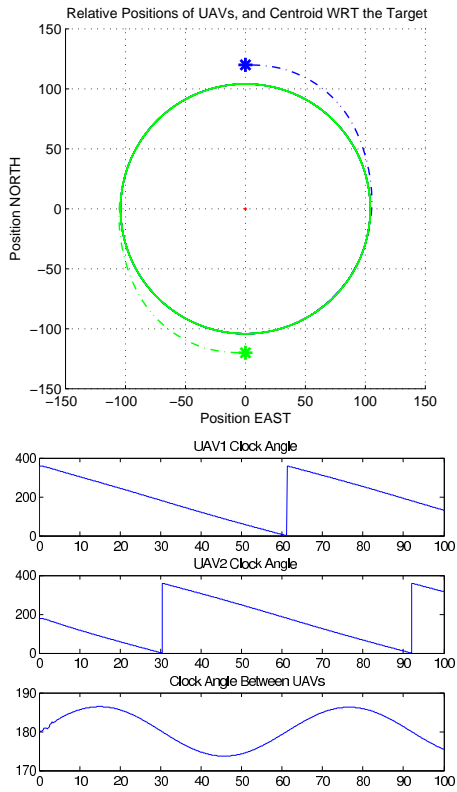
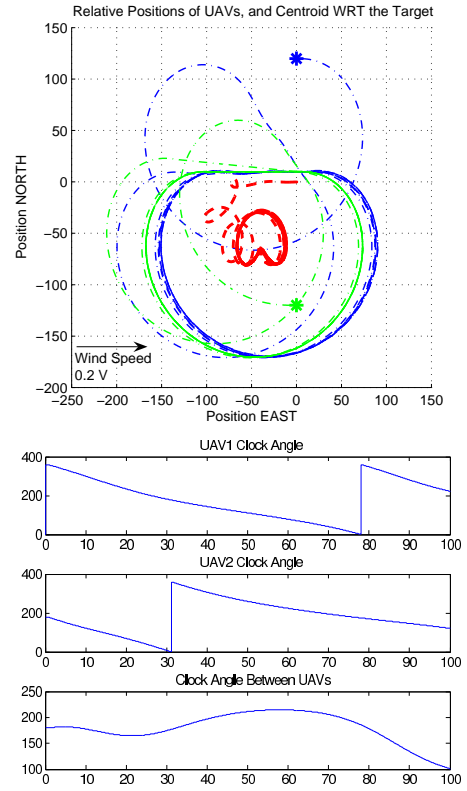**Figure 28.** **Centroid: Tracking a Fixed Target**

Figure 29. **Centroid: Tracking a Fixed Target With Wind**
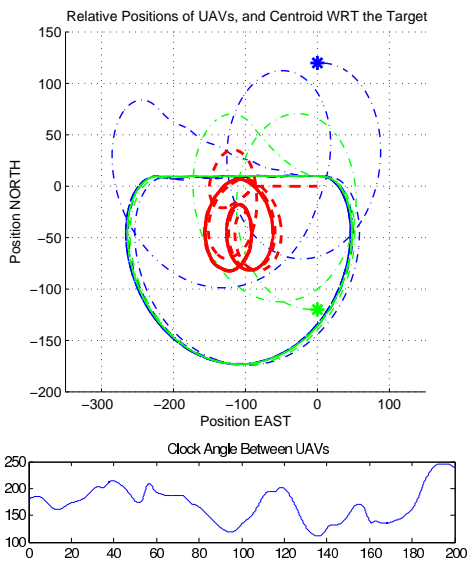

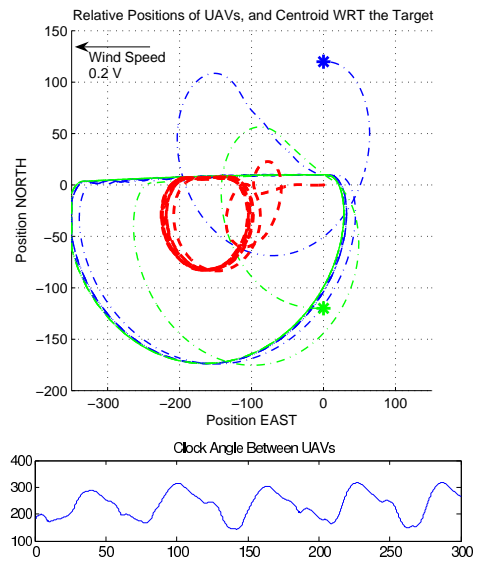**Figure 30.** **Centroid: Tracking a Slow Target**

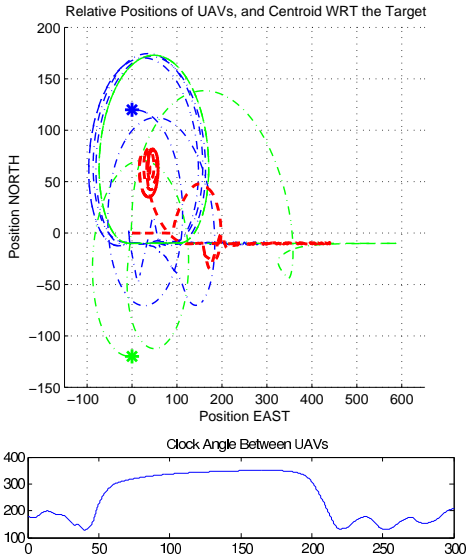**Figure 31.** **Centroid: Tracking a Slow Target With Wind**

16

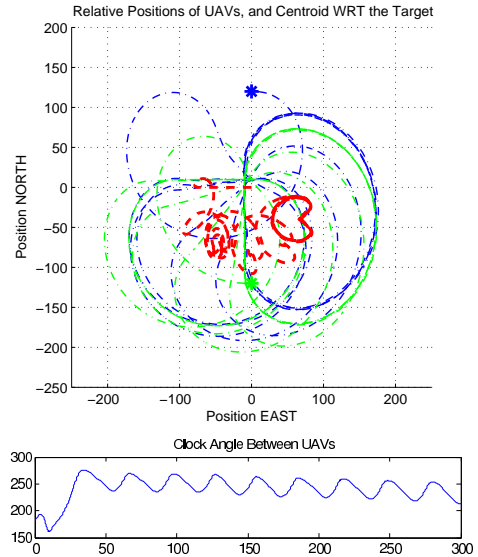**Figure 32. Centroid: Tracking a Fast Target**

Figure 33. Centroid: Tracking a Turning Target

with respect to the target. Maintaining the centroid on the target is the key to keeping angular separation of the UAVs with respect to the target.

Notice that the tangent swarming function keeps the UAVs within range of the fast target in Figure [32] and allows them the regain their orbit when the target slows per the profile in Figure [7]. Also note that in Figure [33], the slower target speed has reduced the clock angle oscillation amplitude, although now a clear drift in average clock angle separation can be detected.

VI.   Method 4 : 'Real-Time' Optimization for Predictive Control

There are many fast and efficient routines for solving optimization problems, particularly if the space over which to optimize is convex [1]. If the optimization can be done fast enough, given computational limits, it can be used in concert with Model Predictive Control to accurately determine future commands.

A.   Using Model Predictive Control

Let time now $= T$ and the current command $= \theta_c(T)$. Due to calculation time (δ_t), the next command will be available at time $T + \delta_t$. If $\delta_t \leq t_f$, then at each integer multiple of t_f, a new command $(\theta(T + n\, t_f))$ will be available for use. See Figure [34]. A zero-order hold can then be used to create a piece-wise constant command. $\theta_c(t)$.

B.   Formulating Tracking as Model Predictive Control

Target and/or wind speed will affect UAV relative position and speed with respect to the target. Given this effect, the control input that results in the desired relative future position and speed of the UAV can be precisely determined. This assumes UAV, target, and wind field dynamics and their interactions are known accurately from current time until the future time. Figure [35] graphically shows how UAV position changes relative to the target as the target moves over a small time increment. Here, the target moves incremental lengths dTx and dTy. The UAV, starting from position 1 has a clock angle δ. The UAV moves length dU (angle α) in the absolute frame and dR (angle $\alpha + \beta$) in the relative frame, resulting in a clock angle γ. Note that relative position 2 remains a distance R from the target. Therefore, neglecting dynamics, α represents the commanded heading the UAV must have had at position 1 to get to position 2. Given dTx, dTy, R, and δ, α (and dR, β, γ) can be found by solving the following set of equations:
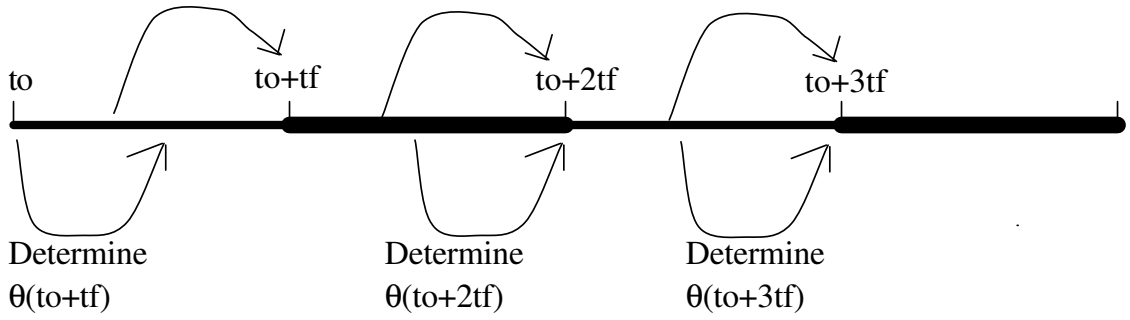
$$dR\cos(\alpha + \beta) = dU\cos\alpha - dtx$$

17

Figure 34. Calculation and Data Flow

$$dR \sin(\alpha + \beta) = dU \sin \alpha - dty$$
$$R \cos \gamma + dR \cos(\alpha + \beta) = dtx + R \cos \gamma$$
$$R \sin \gamma + dR \sin(\alpha + \beta) = dtx + R \sin \gamma \tag{15}$$

Note, this set is solved as an optimization problem by moving all terms in each equation to right side. The equation solution would cause each right hand side to evaluate to zero. The optimization is to minimize the norm of the function evaluations. If the norm is zero, the the optimal set found is also the solution to the equation set.

Note also that the wind effect on relative speed can be included by modifying dTx and dTy to include the relative effects of wind in the x and y directions, respectively. For example, if the wind is adverse to the UAV in the x-direction, dTx would increase accordingly.

By solving for α at small time steps Δt in length, it is reasonable to assume that the target and wind
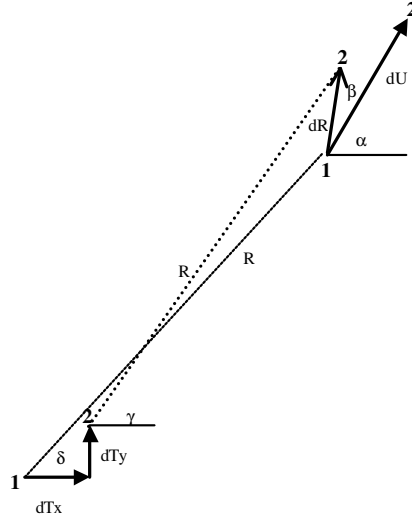

Figure 35. Relative Motions

velocities are constant over Δt. Therefore, $dTx = V_{tx}\Delta t$ and $dTy = V_{ty}\Delta t$. To convert to a heading rate command, the heading rate is assumed proportional to the difference in subsequent calculations of heading:

$$\dot{\alpha} = k_1(\alpha - \alpha^-) \tag{16}$$

18

To account for initial condition errors, the heading rate is modified by assuming the UAV is always driving to maintain commanded stand-off distance:

$$\dot{\alpha}_c = \dot{\alpha} + k_2(R_c - R)/R \tag{17}$$

C.   Commanding Speed to Achieve Angular Separation

Along the same reasoning as the Lyapunov method, angular separation is achieved by varying UAV speed proportional to the angular separation error:

$$\Delta V_c = k_3(\Psi_c - (\Psi_1 - \Psi_2)) \tag{18}$$

Note that k_3 is negative for UAV1 and positive for UAV2. Therefore, the vehicles will change speeds equally but oppositely (one will increase, the other decrease).
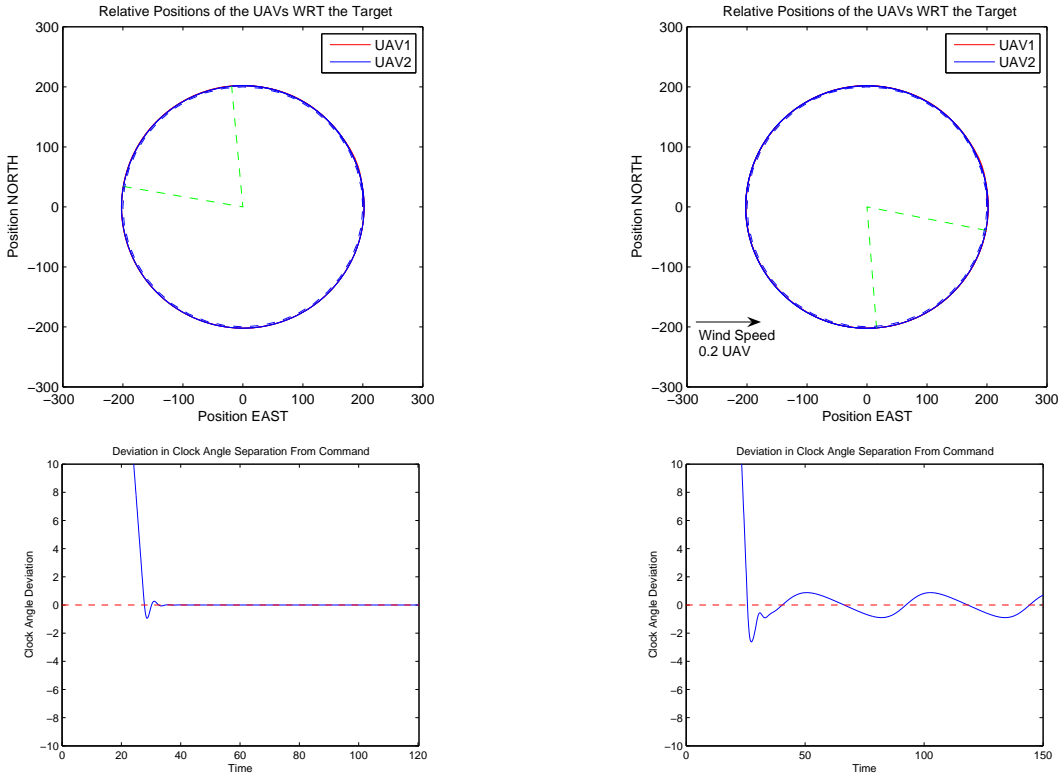
D.   Simulations

Figure 36. RTO: Tracking a Fixed Target

Figure 37. RTO: Tracking a Fixed Target With Wind

Figures [36-41] resulted as the target and wind velocity profiles were changed per Section [II.6].

Figure [36] demonstrates that this method can quickly achieve and maintain a loitering orbit about a stationary target. The response time is similar to the Helmsman method. The introduction of wind results in only a small oscillation as seen in Figure [37].

When the target speed is slow, Figure [38] shows that the motion creates an unsteady, but still small oscillation of ± 5 degrees, or twice the Lyapunov method. However, the introduction of an adverse wind (see Figure [39]) eventually results in unstable behavior in the follower UAV. Note that this behavior starts when the lead UAV is at its lowest relative speed (most Southerly point on the relative orbit). The velocity compensation is not enough to account for both the adverse wind and the target. The radius of the follower
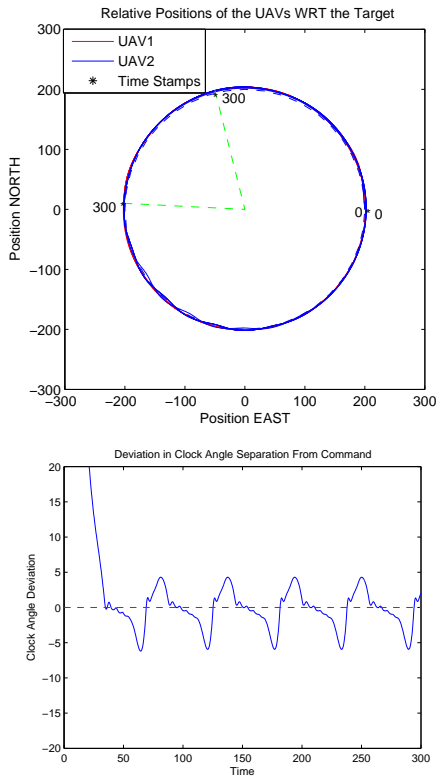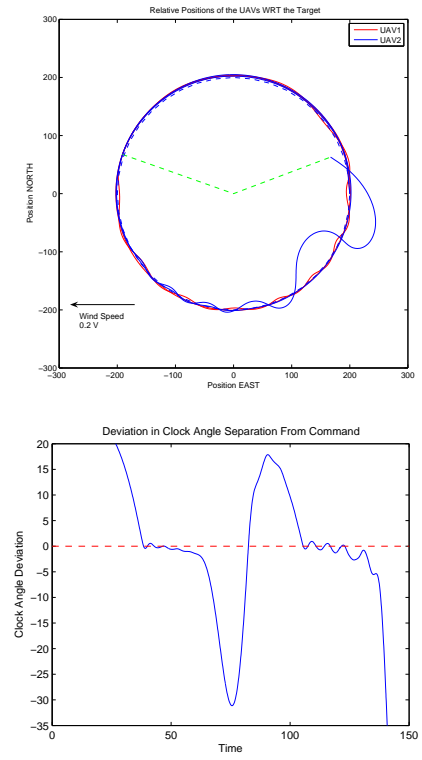
19

Figure 38. RTO: Tracking a Slow Target

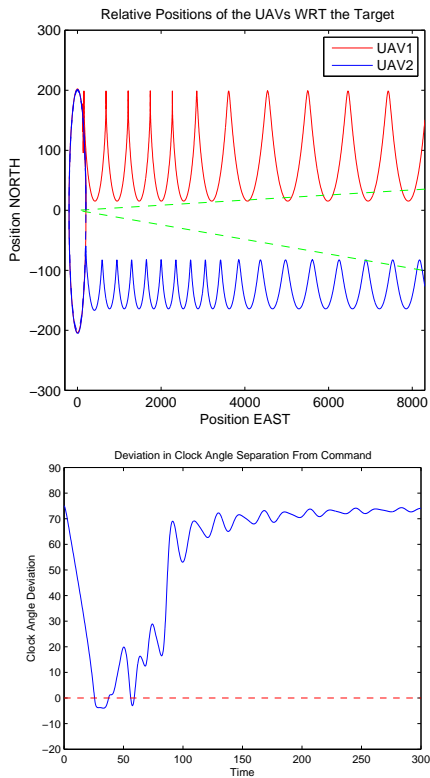**Figure 39. RTO: Tracking a Slow Target With Wind**
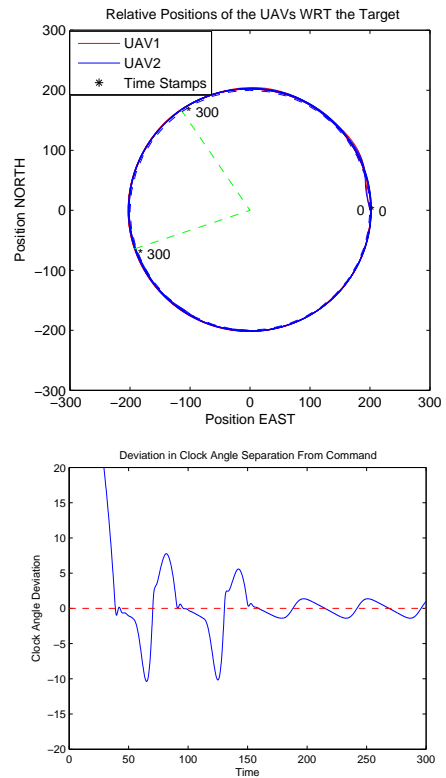

Figure 40. RTO: Tracking a Fast Target

Figure 41. RTO: Tracking a Turning Target

UAV begins to oscillate, effectively slowing its clock angle rate. The radius compensation is taxed to keep the UAV near the specified stand-off distance and starts to overshoot considerably. By the time the follower UAV reaches its lowest relative speed, the clock separation has started to diverge quickly. This quickens the overshoots towards instability.

As stated, this method cannot work for target speeds faster than the lowest UAV speed. As an example, Figure [40] shows the unstable behavior resulting from the fast target profile.

Finally, tracking a target through a turn is demonstrated in Figure [41]. The result is similar to a the slow target in Figure [38], but with lower steady oscillations, as this target is slower. The oscillation amplitude is almost exactly the same as in Figure [37], which has wind speed the same magnitude as the turning target.

VII.   Conclusion

This paper investigated four low heuristic methods for coordinated tracking of a moving target. The following summarizes the advantages and disadvantages of the each method.

Good Helmsman Behavior

- This method works the best to maintain relative clock angle and could be improved, possibly, by commanding relative angle smaller as target or wind speed increases.

- Anti-windup methods are necessary to prevent command saturation

- This method does not take into account a target faster than the UAVs. If the initial conditions are significantly different from the desired orbit, convergence to the orbit occurs, but is slow.

Modified Lyapunov Vector Field

- This method produces feasible commands (within the capability of the UAV), at least when wind is not present.

- The relative clock angle between the two UAVs oscillates whenever the target or wind speed is non-zero.

- The tangent method works well as a command when the UAV is distant from the target, such as when the target moves faster than the UAV.

Controlled Collective Motion

- This method works well for three, and possibly more, vehicles. For two, a possible solution was given. However, this solution had the least ability to maintain target clock angle.

- Wind is very detrimental to this method.

- Considerable work must still be done to integrate the logic of this work, based on an oscillator model, onto a real UAV.

'Real-Time' Optimization

- As is common with predictive control, this method depends heavily on the model used to propagate commands. Feedback is necessary to keep initial conditions near the 'expected' values.

- Velocity compensation for clock angle separation can lead to unstable behavior at high wind and/or target speeds.

- This type of method, if needed to run in actual 'real-time', would require considerable computing power to perform the optimization quick enough to output the needed commands.

Any method that is to work well must account for the wind and a target that, at least for some time, can outperform the UAV.

Acknowledgments

References

[1]Boyd, S. and Vandenberghe, L."Convex Optimization", Cambridge University Press, 2004.

[2]Campbell, M. and Ousingsawat, J. "On-line Estimation and Path Planning for Multiple Vehicles in an Uncertain Environment", AIAA Guidance, Navigation, and Control Conference, Monterey, CA, August 2002.

[3]Frew, E. and Lawrence, D., "Cooperative Stand-off Tracking of Moving Targets by a Team of Autonomous Aircraft", AIAA Guidance, Navigation, and Control Conference, San Francisco, CA, August 2005.

[4]Klein, D. and Morgansen, K., "Controlled Collective Motion for Trajectory Tracking", Proceedings of the American Control Conference, 2006.

[5]Lawrence, D., "Lyapunov Vector Fields for UAV Flock Coordination", 2nd AIAA "Unmanned Unlimited" Aerospace Sytems, Technology, and Operations Conference, San Diego, CA, August 2002.

[6]Ogren, P. and Egerstedt, M., "A Control Lyapunov Function Approach to Multiagent Coordination," IEEE Transactions of Robotics and Automation, Vol 18, No. 5, OCT 2002.

[7]Rysdyk, R. "UAV Path Following for Constant Line-of-Sight Target Observation," Journal of Guidance, Navigation, and Control, in press.

[8]S. Stolle and R. Rysdyk, "Flight Path Following Guidance for Unmanned Air Vehicles with Pan-tilt Camera for Target Observation," Digital Avionics Systems Conference, Indianapolis, IN, 2003.